Secondary Control for Distributed Converter Interfaced Generation with Prescribed Transient-state Performance in DC Microgrid

Aili Fan, Jiangong Yang, Yuhua Du, Zhipeng Li, Fei Gao, and Yigeng Huangfu

***Abstract*—In this paper, a set of distributed secondary controllers is introduced that provide active regulation for both steady-state and transient-state performances of an islanded DC microgrid (MG). The secondary control for distributed converter interfaced generation (DCIG) not only guarantees that the system converges to the desired operating states in the steady state but also regulates the state variations to a prescribed transient-state performance. Compared with state-of-the-art techniques of distributed secondary control, this paper achieves accurate steady-state secondary regulations with prescribed transient-state performance in an islanded DC MG. Moreover, the applicability of the proposed control does not rely on any explicit knowledge of the system topology or physical parameters. Detailed controller designs are provided, and the system under control is proved to be Lyapunov stable using large-signal stability analysis. The steady-state and transient-state performances of the system are analyzed. The paper proves that as the perturbed system converges, the proposed control achieves accurate proportional power sharing and average voltage regulation among the DCIGs, and the transient variations of the operating voltages and power outputs at each DCIG are regulated to the prescribed transient-state performance. The effectiveness of the proposed control is validated via a four-DCIG MG system.**

***Index Terms*—Cyber-physical system, distributed control, DC microgrid, prescribed performance control, secondary control.**

I. Introduction

TO coordinate distributed converter interfaced generations (DCIGs) in microgrids (MGs), hierarchical control has been widely adopted. The secondary level of hierarchical control is originally introduced to compensate for steady-state deviations caused by droop control at the primary level. As the operating characteristics of modern power grids have become more complex, secondary controls with advanced control objectives have been extensively studied, e.g., proportional power sharing [1], seamless network reconfiguration [2], and cyber resilience [3]. In recent years, distributed control approaches have been favored over centralized approaches [4], where the secondary regulations are achieved in a decentralized manner.

By far, most existing distributed secondary controls are steady-state-focused (SS-focused), i.e., the MG system is regulated to the desired steady-state operating states as the implemented distributed secondary control converges. Consensus-based algorithms have been frequently adopted in MG control designs [5]. Multiple DCIGs reach consensus when they are controlled to gradually agree on the value of a designed control variable using peer-to-peer information exchange, and the MG system is then regulated to the desired steady-state operating points. In addition, these controls remain effective as the operating conditions of the system vary, which ensures that the steady state of the MG system is updated as desired. As the MG system is regulated towards a new steady state, the operating states of the system vary continuously, and the system is in a transient state. Conventional SS-focused distributed secondary controls are not dedicated to handle the transient responses of the system properly [6] because conventional power systems are rich in load diversity. In other words, because of their diverse patterns and features, not all loads run at full capacity simultaneously. Thus, the overall load variations within the grid would be relatively smooth. However, MG systems are known for their lack of both inertia and load diversity [7] and thus are susceptible to severe transient distubances [8], e.g., inrush current/voltage, that can lead to false operation of protection, forced DCIG disconnection, etc. Thus, it is critical to implement distributed secondary controls that are transient-state-focused in MG systems.

The transient-state performance of DCIGs has been extensively studied. The main focus of the related research works can be classified as voltage-controlled-mode DCIGs that operate as virtual synchronous generators [9] or that adopt droop control [10]; current-controlled-mode DCIGs that synchronize with the grid using a phase-locked loop [11]; and hybrid systems with both voltage- and current-controlled-mode DCIGs in parallel [12]. However, these approaches are

Manuscript received: March 12, 2024; revised: June 30, 2024; accepted: October 8, 2024. Date of CrossCheck: October 8, 2024. Date of online publication: November 15, 2024.

This work was supported in part by Fundamental Research Funds for the Central Universities, Northwestern Polytechnical University, and in part by Xianyang Key R&D Program (No. L2023-Z DYF-QYCX-012)

This article is distributed under the terms of the Creative Commons Attribution 4.0 International License (http://creativecommons.org/licenses/by/4.0/).

A. Fan, J. Yang, Y. Du (corresponding author), and Y. Huangfu are with School of Automation, Northwestern Polytechnical University, Xi'an 710129, China (e-mail: ailifan@ieee. org; jiangong. yang@mail. nwpu. edu. cn; yuhua. du@ieee.org; yigeng@nwpu.edu.cn).

Z. Li is with Institute of Flexible Electronics, Northwestern Polytechnical University, Xi'an 710129, China (e-mail: iamzpli@nwpu.edu.cn).

F. Gao is with University of Technology of Belfort-Montbéliard, CNRS, Institut FEMTO-ST, F-90010 Belfort cedex, France (e-mail: fei.gao@utbm.fr).

DOI: 10.35833/MPCE.2024.000267

mainly stability-oriented and not designed to provide active regulations over the transient responses of the system. To ensure guaranteed transient responses for DCIGs within a wide operating range, adaptive control approaches have been employed in many research works, wherein the control gains are fine-tuned on the fly to regulate the operating states of DCIGs during the transient state [13]-[15]. These approaches deal with the interactions between the individual DCIG and the external grid during the transient state. However, they cannot effectively handle the interactions among multiple DCIGs within an islanded MG.

Communication-less controls have been favored to enhance the transient-state performance of an islanded MG energized by multiple DCIGs [16]. Decentralized control approaches have been adopted in many research works [17]-[21], where the transient responses of the DCIGs are coordinately mitigated using only local measurements. However, these controls are generally model-dependent, and their performances cannot always be guaranteed when the MG systems operate under time-varying topologies and plug-and-play DCIGs. Unlike under decentralized control approaches, distributed control approaches can access global information indirectly through a communication network with sufficient connectivity, which gives them additional controllability. Finite-time and fixed-time consensus algorithms have been frequently utilized to achieve distributed MG secondary control with a prescribed convergence time during the transient state [22]-[24]. However, the convergence rate is usually accelerated at the expense of overshoot in most consensus-based algorithms, which may lead to undesirable transient responses.

Prescribed performance controls (PPCs) have recently been studied to achieve distributed MG secondary control with rapid convergence and overshoot suppression. Compared with stability-oriented approaches [25]-[27], these controls ensure that the regulation errors of particular states are always within predefined bounds during the transient state. In [28], a set of distributed controllers is developed that achieves optimal DCIG dispatch while ensuring a bounded DCIG operating voltage during both the transient state and steady state. However, the voltage regulation is effective only during the optimal dispatch regulation at the tertiary control level and cannot handle the transient responses caused by load disturbances at the secondary control level. In [29], a compromised controller design is proposed that achieves both voltage regulation and current sharing among the DCIGs, where a tradeoff exists between the tightness of voltage bounding and current-sharing errors. A flexible yet prescribed regulation over the operating voltage of each DCIG is achieved, but its focus is only on the steady state. In [30], a containment-based distributed control approach is developed that guarantees that the voltage of each DCIG is continuously regulated within predefined bounds while achieving proper average voltage regulation at a steady state. However, the developed control relies on the measurement and transmission of real-time voltage derivations at each DCIG, which are difficult to implement.

In [31], a distributed secondary control scheme is developed for islanded DC MG operation, and the evolution of both the bus voltage error and current-sharing error is always constrained within a predefined bound. However, this research work is applicable only to DC MGs with a single aggregated load bus, and accurate knowledge of the transmission lines is required, which is difficult to realize in practice. A distributed control approach for islanded AC MG operation with the expected dynamic performance is proposed in [32], where the expected state convergence and overshoot suppression performance could be achieved. Although [32] focuses on AC MG, its voltage regulation approach can also be adopted for DC MG, albeit with random steady-state deviations. Compared with secondary frequency regulation, secondary voltage restoration in DC MGs presents additional challenges. This is because voltage is not globally uniform as the MG system in a steady state.

In this paper, a distributed secondary control with prescribed transient-state performance is proposed to coordinate multiple DCIGs in an islanded DC MG. The proposed control achieves accurate average voltage regulation and proportional power sharing among DCIGs in the steady state and achieves prescribed dynamic performance during the evolution of the DCIG operating voltage and power output in the transient state. In addition to achieving the regular MG secondary control objectives, the proposed control provides adaptive overshoot suppression of the voltage transients at each DCIG, which can improve the overall transient responses within the MG. Compared with state-of-the-art approaches [31], [32], this paper has the following notable features: it requires neither accurate knowledge of the system parameters nor is restricted by the grid topology; moreover, no steady-state deviations are observed. The proposed control is implemented on an original control framework that couples the cyber network and physical network, and detailed controller designs are presented. The Lyapunov stability of the proposed control is verified. The effectiveness of the proposed control under steady states and transient states is analyzed and validated via a four-DCIG MG system in Simulink/MATLAB.

II. Preliminaries

A. Developed Cyber-physical System (CPS) Control Framework

The converter-dominated MG system under distributed control forms a CPS, where the droop-controlled DCIGs in the physical network are represented as intelligent agents implemented with distributed control protocols in the cyber network. The cyber network is modeled as a connected and undirected graph, $G=(V,\varepsilon)$, where $V=\{v_1,v_2,\ldots,v_N\}$ denotes the set of DCIGs and $\varepsilon\subseteq V\times V$ denotes the valid communication links between the DCIGs. In addition, for $v_i\in V$, at least one $v_j\in V\ (i\neq j)$ exists such that $\{v_i,v_j\}\in\varepsilon$. The Laplacian matrix of the cyber network G is defined as $\boldsymbol{L}=\boldsymbol{D}-\boldsymbol{A}$, where $\boldsymbol{A}=(a_{ij})$ is the adjacency matrix that is symmetric and defined as $a_{ij}=a_{ji}=1$ if and only if the edge $\{v_i,v_j\}\in\varepsilon$,

otherwise, $a_{ij}=a_{ji}=0$, and $\boldsymbol{D}=\mathrm{diag}(d_{ii})$, where $d_{ii}=\sum_{j=1}^{n}a_{ij}$.

The interaction between each DCIG and its representative agent is usually realized by a constant shift in the droop curve as the distributed controller converges, which is also known as the secondary control variable [33]. As previously discussed, this type of control framework mainly focuses on the steady-state performance of the system. To introduce proper regulation efforts during both steady state and transient state, a CPS control framework is developed and expressed as:

$$\dot{v}_i(t)=-k_iP_i(t)+u_i(t) \tag{1a}$$

$$\dot{P}_i(t)=\frac{1}{\tau}\left(v_i(t)i_i(t)-P_i(t)\right)+d_i(t) \tag{1b}$$

$$\dot{\bar{v}}_i(t)=-k_p\sum_{j=1}^{N}a_{ij}\left(k_iP_i(t)-k_jP_j(t)\right)-k_v\left(V_i(t)-V^*\right) \tag{1c}$$

$$\dot{V}_i(t)=\dot{v}_i(t)-k_V\sum_{j=1}^{N}a_{ij}\left(V_i(t)-V_j(t)\right) \tag{1d}$$

where the subscript i denotes the i^{th} DCIG; $v_i(t)$ and $i_i(t)$ are the DCIG operating voltage and current, respectively; $P_i(t)$ is the measured DCIG output power; k_i and k_j are the droop gains; k_p, k_v, and k_V are the secondary control gains; τ is the time constant for power filter; V^* is the rated voltage; $\bar{v}_i$ is the virtual voltage that has no physical significance; V_i and V_j are the estimated average DCIG voltages using a dynamic consensus algorithm; and $u_i(t)$ and $d_i(t)$ are the designed control inputs, the detailed designs of which are next examined.

As shown in (1b), compared with the conventional power measurement technique in which a first-order low-pass filter is adopted, the designed control input $d_i(t)$ introduces additional regulation efforts. Notably, instead of the conventional V-P droop, $\dot{V}$-P droop is adopted in (1a) as the primary control [34]. Moreover, (1d) is developed in the standard form of a dynamic consensus algorithm, and the following relationship is obtained [35] as $V_i(t)=\frac{1}{N}\sum_{i=1}^{N}v_i(t)$ when $t\to\infty$. Finally, by setting $u_i(t)=\bar{v}_i$ and $d_i(t)=0$, we reduce the developed control framework in (1) to the SS-focused conventional distributed secondary control algorithm, thus indicating the extended control flexibility of the developed CPS control framework.

B. Prescribed Performance

The concept of prescribed performance has been studied extensively in robotics and aviation. In subsequent discussions, the error between two bounded states $e(t)$ is said to have a prescribed performance if it converges to an arbitrarily small residue and exhibits an overshoot less than a prespecified constant [36].

Conventionally, a smooth function $\rho(t)$ is called a performance function if it has the following properties:

1) $\rho(t)$ is positive and decreasing for $t\geq 0$.

2) $\lim_{t\to 0}\rho(t)=\rho_0>0$, $\lim_{t\to\infty}\rho(t)=\rho_\infty>0$, and $\rho_0>\rho_\infty>0$.

In addition, the prescribed performance of $e(t)$ is satisfied when $-\delta\rho(t)<e(t)<\rho(t)$, if $e(t)>0$; and $-\rho(t)<e(t)<\delta\rho(t)$, if $e(t)<0$; where $0\leq\delta\leq 1$, and ρ_∞ represents the maximum allowable error $e(t)$ in the steady state. The aforementioned statements regarding the conventional performance function are illustrated in Fig. 1.

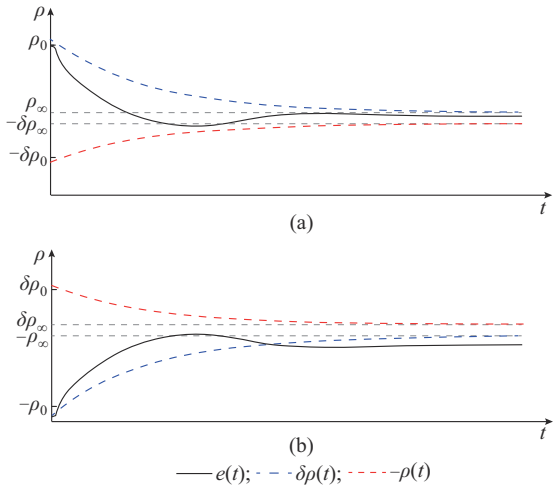

Fig. 1. Representations of prescribed performance of $e(t)$ with decaying performance function. (a) $e(t)>0$. (b) $e(t)<0$.

Notably, in the conventional PPC problem, the system is initially perturbed and the decaying performance function is activated simultaneously. However, the MG system under study initially operates in a steady state, and the transients are introduced due to unplanned events at random time instants, which makes it challenging to re-activate the performance function, i.e., re-set $\rho(t)$ to ρ_0 every time the transients are detected. To implement PPC in the control of the MG system with continuous regulations over the transient responses of the MG system, the performance function in the subsequent analysis is set to be constant (or with an extremely slow decaying rate). This ensures that the performance function is not repetitively reactivated and the MG system operates with the prescribed transient-state performance. The aforementioned statements regarding the adopted performance function are illustrated, as shown in Fig. 2, where $\delta=1$ is set for generality. In addition, the transients caused by unplanned events are generated at time instants t_1 and t_2 when the system is in the steady state as $e(t)=e_{ss}$, and the variations of $e(t)$ are bounded within the constant range $[-\rho,\rho]$ as prescribed.

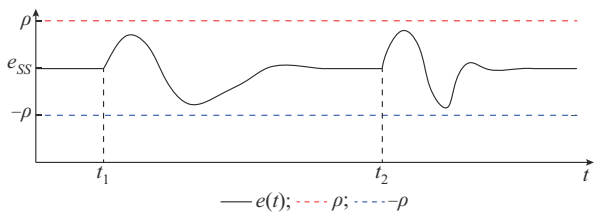

Fig. 2. Representations of prescribed performance of $e(t)$ with adopted constant performance function.

C. Control Objectives

As previously discussed, to properly coordinate multiple DCIGs in an islanded DC MG with overall transient response of the improved system, the control objectives of the proposed control are designed as follows:

1) In the steady state, proportional power sharing among DCIGs is achieved and the average DCIG voltage is regulated as rated, i.e., for the i^{th} DCIG and when $t\to\infty$: $k_iP_i(t) = k_jP_j(t)$ and $\frac{1}{N}\sum_{i=1}^{N}v_i(t) = V^*$.

2) In the transient state, the tracking errors between the virtual and operating voltages at each DCIG are constrained. The same is true of the normalized power-sharing errors at each DCIG i. e., for the i^{th} DCIG and when $t>0$: $\left|\bar{v}_i(t) - v_i(t)\right| \le \rho_{v,i}$ and $\left|\frac{1}{d_{ii}}\sum_{j=1}^{N}a_{ij}\left(k_iP_i(t) - k_jP_j(t)\right)\right| \le \rho_{p,i}$, where $\rho_{v,i}>0$ and $\rho_{p,i}<0$ are the designed parameters.

The steady-state control objectives have been extensively discussed in the literature and therefore are not discussed further herein. Both control objectives in the transient state are designed to enable rapid convergence and overshoot suppression of the voltage transients at each DCIG, because the dynamic couplings between the voltage and power flow within an islanded DC MG can improve the overall transient responses of the system. Specifically, referring to (1a) and (1b), the following can be obtained.

1) Condition $\left|\bar{v}_i(t) - v_i(t)\right| \le \rho_{v,i}$ indicates that at each DCIG, its operating voltage $v_i(t)$ is bounded by a time-varying boundary defined by $\bar{v}_i(t)$, with a pre-defined margin $\rho_{v,i}$. A prescribed performance regarding the DCIG operating voltage is thus enabled, which represents a direct regulation over the voltage transients and thus over the overall dynamics of the MG system.

2) Condition $\left|\frac{1}{d_{ii}}\sum_{j=1}^{N}a_{ij}\left(k_iP_i(t) - k_jP_j(t)\right)\right| \le \rho_{p,i}$ indicates that at each DCIG, the normalized power output $k_iP_i(t)$ is bounded by a time-varying boundary defined by $\frac{1}{d_{ii}}\sum_{j=1}^{N}a_{ij}k_jP_j(t)$, with a predefined margin $\rho_{p,i}$. Thus, the prescribed performance for the measured DCIG output power is achieved. Recall the dynamic couplings between $v_i(t)$ and $P_i(t)$ in (1a); this condition represents an indirect regulation over the voltage transients but could still improve the overall dynamics.

Notably, as the MG system under control converges, the designed control objectives in the transient state are reduced to $\bar{v}_i(t) = v_i(t)$ and $k_iP_i(t) = k_jP_j(t)$ for $i,j = 1, 2, \ldots, N$, which are not in conflict with the designed control objectives in the steady state. Also noteworthy is the fact that unlike the conventional boundaries that are predefined, the developed boundaries for both the DCIG operating voltage and power output regulations vary with the system operating states, which would result in extended applicability. Further discussion regarding the system performance in both steady and transient states is provided in subsequent sections. Finally, the feasibility of the transient-state control objectives is mainly determined by the selection of $\rho_{v,i}$ and $\rho_{p,i}$. As previously discussed, these parameters represent the designed margins between the operating states of the DCIG and their developed time-varying boundaries. Thus, greater values of $\rho_{v,i}$ and $\rho_{p,i}$ could lead to extended control feasibility. Note that advanced design principles of $\rho_{v,i}$ and $\rho_{p,i}$ are out of the scope of this paper.

III. Proposed Controller Design

Under the developed CPS control framework as described by (1), to fulfill the designed control objectives, the control inputs $u_i(t)$ and $d_i(t)$ are expressed as:

$$u_i(t) = -k_p\sum_{j=1}^{N}a_{ij}\left(k_iP_i(t) - k_jP_j(t)\right) - k_v\left(V_i(t) - V^*\right) + k_iP_i(t) + \alpha_iQ_i(t)\xi_i(t) \tag{2a}$$

$$d_i(t) = \frac{1}{k_id_{ii}}\sum_{j=1}^{N}a_{ij}k_j\dot{P}_j(t) - \frac{\beta_i}{\tau}\Delta_i(t)\left(v_i(t)i_i(t) - P_i(t)\right) - \gamma_i\frac{1-\beta_i}{\tau}\Delta_i(t)\,sgn\left(\zeta_i(t)\right)\left(P_i(t) + v_i(t)i_i(t)\right) - \beta_i\Delta_i(t)\zeta_i(t) \tag{2b}$$

where $\alpha_i>0$, $1>\beta_i>0$, and $\gamma_i>0$ are the designed positive scalars; $sgn(\cdot)$ is the sign function; and $Q_i(t)$, $\xi_i(t)$, $\Delta_i(t)$, and $\zeta_i(t)$ are the designed transient control terms.

$$Q_i(t) = \frac{1}{\Phi_{v,i}^{-1}\left(\xi_i(t)\right) + \rho_{v,i}} - \frac{1}{\Phi_{v,i}^{-1}\left(\xi_i(t)\right) - \rho_{v,i}} \tag{3a}$$

$$\xi_i(t) = \Phi_{v,i}\left(\bar{v}_i(t) - v_i(t)\right) \tag{3b}$$

$$\Delta_i(t) = \frac{1}{\Phi_{p,i}^{-1}\left(\zeta_i(t)\right) + \rho_{p,i}} - \frac{1}{\Phi_{p,i}^{-1}\left(\zeta_i(t)\right) - \rho_{p,i}} \tag{3c}$$

$$\zeta_i(t) = \Phi_{p,i}\left[\frac{1}{d_{ii}}\sum_{j=1}^{N}a_{ij}\left(k_iP_i(t) - k_jP_j(t)\right)\right] \tag{3d}$$

where the functions $\Phi_{v,i}(x)$ and $\Phi_{p,i}(x)$ are inspired by the celebrated PPC from [36] and defined as: $\Phi_{v,i}(x) = \frac{1}{2}\ln\frac{\rho_{v,i}+x}{\rho_{v,i}-x}$; $\Phi_{v,i}^{-1}(x) = \frac{\rho_{v,i}e^{2x} - \rho_{v,i}}{1+e^{2x}}$; $\Phi_{p,i}(x) = \frac{1}{2}\ln\frac{\rho_{p,i}+x}{\rho_{p,i}-x}$; and $\Phi_{p,i}^{-1}(x) = \frac{\rho_{p,i}e^{2x} - \rho_{p,i}}{1+e^{2x}}$.

Equation (2) shows that, based on conventional SS-focused control, the implementation of the proposed controller does not have additional installation requirements and it does not rely on accurate knowledge of system parameters and is applicable to general grid topologies. Figure 3 shows the control flow of the proposed controller, where its performance is analyzed in detail in the following sections. Notably, with reference to (1)-(3), in the case that one DCIG is completely isolated from the remaining DCIGs due to extreme communication failures, the faulted DCIG operates under droop control and contributes to the stabilization of the system, whereas the remaining DCIGs keep coordinated and provide proper regulation.

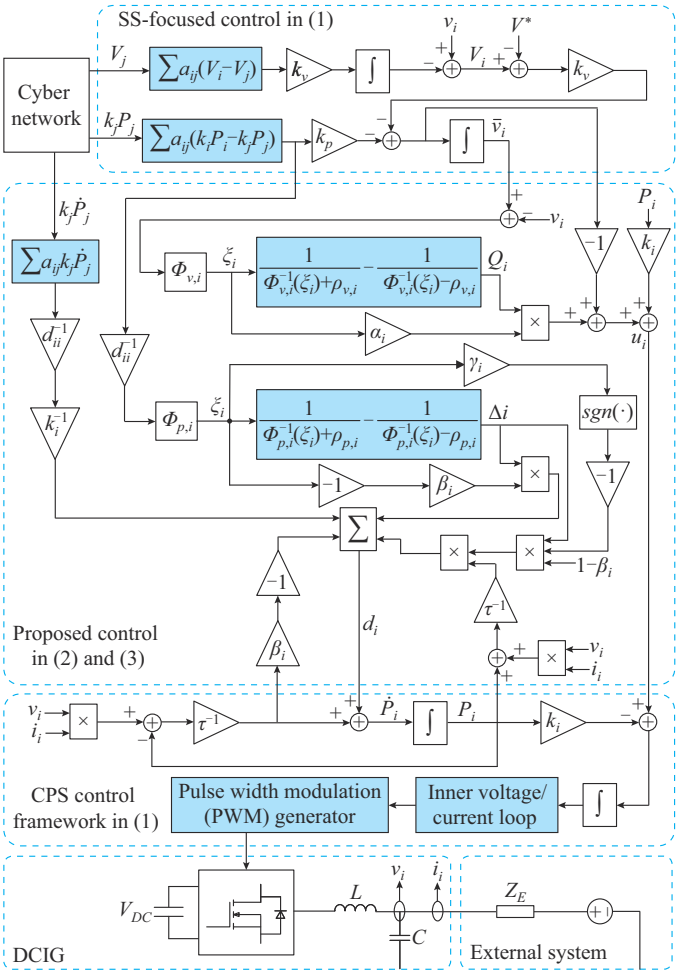

Fig. 3. Control flow of proposed controller under developed CPS control framework.

The stability of the developed control input $u_i(t)$ in (2a) is proven by constructing the following Lyapunov function:

$$W_1(t)=\sum_{i=1}^{N}\xi_i^2(t)\geq 0 \tag{4}$$

Referring to (1a), (1c), and (2a), we derive $W_1(t)$ as:

$$\begin{aligned}\dot{W}_1(t)&=2\sum_{i=1}^{N}\xi_i(t)\dot{\xi}_i(t)=2\sum_{i=1}^{N}\xi_i(t)\frac{1}{2}Q_i(t)\left(\dot{\bar{v}}_i(t)-\dot{v}_i(t)\right)=\\&\sum_{i=1}^{N}\xi_i(t)Q_i(t)\left[-k_p\left(k_iP_i(t)-\bar{P}_i(t)\right)-k_v\left(V_i(t)-V^*\right)-\right.\\&\left.\left(-k_iP_i(t)+u_i(t)\right)\right]=-\sum_{i=1}^{N}\alpha_iQ_i^2(t)\xi_i^2(t)\leq 0\end{aligned} \tag{5}$$

Similarly, the following Lyapunov function is constructed to prove the stability of $d_i(t)$ in (2b):

$$W_2(t)=2\sum_{i=1}^{N}\zeta_i^2(t)\geq 0 \tag{6}$$

Referring to (1b) and (2b), we derive $W_2(t)$ as:

$$\begin{aligned}\dot{W}_2(t)&=\sum_{i=1}^{N}\zeta_i(t)\dot{\zeta}_i(t)=2\sum_{i=1}^{N}\zeta_i(t)\frac{1}{2}\Delta_i(t)\left(k_i\dot{P}_i(t)-\right.\\&\left.\frac{1}{d_{ii}}\sum_{j=1}^{N}a_{ij}k_j\dot{P}_j(t)\right)=\sum_{i=1}^{N}\gamma_ik_i\frac{1-\beta_i}{\tau}\zeta_i^2(t)\Delta_i^3(t)\cdot\\&\left[-P_i(t)\left(1+sgn\left(\zeta_i(t)\right)\right)+v_i(t)i_i(t)\left(1-sgn\left(\zeta_i(t)\right)\right)\right]\end{aligned} \tag{7}$$

In the next section, we prove that $\Delta_i(t)>0$ for $t>0$. Given that the DCIGs under study guarantee that $v_i(t)i_i(t)>0$ and $P_i(t)>0$, and when we also recall that $1>\beta_i>0$ and $\gamma_i>0$ by design, the following statements regarding $\dot{W}_2$ can be made as:

1) When $\zeta_i(t)>0$, $\dot{W}_2=-2\sum_{i=1}^{N}\left(1-\beta_i\right)\frac{k_i}{\tau}\zeta_i^2(t)\Delta_i^3(t)P_i(t)<0$.

2) When $\zeta_i(t)=0$, $\dot{W}_2=0$.

3) When $\zeta_i(t)<0$, $\dot{W}_2=-2\sum_{i=1}^{N}\left(1-\beta_i\right)\frac{k_i}{\tau}\zeta_i^2(t)\Delta_i^3(t)v_i(t)\cdot i_i(t)<0$.

We observe that $\dot{W}_2\leq 0$. Referring to (5) and (7), we prove that the MG system under control is Lyapunov stable with the developed control inputs $u_i(t)$ and $d_i(t)$.

Notably, with reference to (1)-(3), only two variables are exchanged among the DCIGs through peer-to-peer communication links, i.e., $P_i(t)$ and $V_i(t)$. This data exchange would not pose a significant burden on the communication bandwidth and could be achieved by state-of-the-art techniques of distributed MG control [37].

IV. Performance Analysis

A. Steady-state Performance Analysis

The stability of the proposed control was demonstrated in the previous section. To further analyze the steady-state performance of the MG system under regulation, the following theorem is proposed.

Theorem 1 For $t>0$, $Q_i(t)>0$ and $\Delta_i(t)>0$, as the system described in (1)-(3) enters the steady state, $\lim_{t\to\infty}\xi_i(t)=0$ and $\lim_{t\to\infty}\zeta_i(t)=0$.

Proof Referring to (3) and the definitions of function $\Phi_{v,i}(x)$ and $\Phi_{p,i}(x)$, we can further express $Q_i(t)$ and $\Delta_i(t)$ as:

$$\begin{aligned}Q_i(t)=&\frac{1}{\frac{\rho_{v,i}e^{2\xi_i(t)}-\rho_{v,i}}{1+e^{2\xi_i(t)}}+\rho_{v,i}}-\frac{1}{\frac{\rho_{v,i}e^{2\xi_i(t)}-\rho_{v,i}}{1+e^{2\xi_i(t)}}-\rho_{v,i}}=\\&\rho_{v,i}\left(1+e^{2\xi_i(t)}\right)\left(\frac{1}{e^{2\xi_i(t)}}+\frac{1}{2}\right)\end{aligned} \tag{8a}$$

$$\begin{aligned}\Delta_i(t)=&\frac{1}{\frac{\rho_{p,i}e^{2\zeta_i(t)}-\rho_{p,i}}{1+e^{2\zeta_i(t)}}+\rho_{p,i}}-\frac{1}{\frac{\rho_{p,i}e^{2\zeta_i(t)}-\rho_{p,i}}{1+e^{2\zeta_i(t)}}-\rho_{p,i}}=\\&\rho_{p,i}\left(1+e^{2\zeta_i(t)}\right)\left(\frac{1}{e^{2\zeta_i(t)}}+\frac{1}{2}\right)\end{aligned} \tag{8b}$$

where $\rho_{v,i}>0$ and $\rho_{p,i}>0$, $i=1,2,\ldots,N$, and thus $e^{2\xi_i(t)}>0$ and $e^{2\zeta_i(t)}>0$, and we can conclude from (8) that $Q_i(t)>0$ and $\Delta_i(t)>0$ when $t>0$.

We then recall the Lyapunov function $W_1(t)=\sum_{i=1}^{N}\xi_i^2(t)\geq 0$ and $\dot{W}_1(t)=-\sum_{i=1}^{N}\alpha_iQ_i^2(t)\xi_i^2(t)\leq 0$. As the system enters the steady state, we can obtain:

$$\lim_{t\to\infty}\dot{W}_1(t)=-\lim_{t\to\infty}\sum_{i=1}^{N}\alpha_iQ_i^2(t)\xi_i^2(t)=0 \tag{9}$$

where $\alpha_i > 0$ and $Q_i(t) > 0$. Thus, the relationship in (9) is true if and only if $\lim_{t\to\infty} \xi_i(t) = 0$.

Similarly, we can observe from the discussion regarding (7) that as the system enters the steady state, $\lim_{t\to\infty} \dot{W}_2(t) = 0$ if and only if $\lim_{t\to\infty} \zeta_i(t) = 0$. The proof is complete.

Referring to Theorem 1 and the relationships in (1) and (2), we can observe the following relationships when $t \to \infty$:

$$0 = -k_i P_i(t) + u_i(t) \tag{10a}$$

$$0 = \frac{1}{\tau}\left(v_i(t) i_i(t) - P_i(t)\right) + d_i(t) \tag{10b}$$

$$u_i(t) = k_p \sum_{j=1}^{N} a_{ij}\left(k_i P_i(t) - k_j P_j(t)\right) + k_v\left(V_i(t) - V^*\right) + k_i P_i(t) \tag{10c}$$

$$d_i(t) = -\frac{\beta_i}{\tau}\left(v_i(t) i_i(t) - P_i(t)\right) \tag{10d}$$

Furthermore, by substituting (10c) into (10a) and (10d) into (10b), we can obtain the following when $t \to \infty$:

$$0 = k_p \sum_{j=1}^{N} a_{ij}\left(k_i P_i(t) - k_j P_j(t)\right) + k_v\left(V_i(t) - V^*\right) \tag{11a}$$

$$0 = \left(1 - \beta_i\right)\left(v_i(t) i_i(t) - P_i(t)\right) \tag{11b}$$

We can further observe from (11) that when $t \to \infty$:

1) $k_i P_i(t) = k_j P_j(t)$ and $V^* = V_i(t) = \frac{1}{N}\sum_{i=1}^{N} v_i(t)$, indicating that accurate proportional DCIG power sharing and average DCIG voltage regulation are achieved.

2) In addition, $P_i(t) = v_i(t) i_i(t)$, indicating that accurate measurement of the DCIG power output is achieved.

Thus, we can conclude that under the proposed control, the steady-state control objectives as outlined in Section II-C are achieved, and the MG system is regulated to the designed steady-state operating states without deviations.

B. Transient-state Performance Analysis

As previously stated, in addition to achieving accurate secondary regulations in the steady state, the proposed controller ensures the prescribed performance of the operating states of the system during the transient state. The following theorem is proven regarding the transient-state performance of an MG system under regulation.

Theorem 2 As the system described by (1)-(3) is perturbed and enters the transient state, the operating states of the system are guaranteed to vary with the prescribed performance.

Proof Referring to (3b), we can further express $\xi_i(t)$ as:

$$\xi_i(t) = \frac{1}{2}\ln\frac{\rho_{v,i} + \left(\bar{v}_i(t) - v_i(t)\right)}{\rho_{v,i} - \left(\bar{v}_i(t) - v_i(t)\right)} \tag{12}$$

From (12), we observe that when the $\bar{v}_i(t) - v_i(t)$ is bounded, so is $\xi_i(t)$, and this can be further described as:

$$\left|\xi_i(t)\right| \le b_i \tag{13}$$

where $b_i > 0$. Referring to (12) and (13), we can establish the following inequality:

$$-b_i \le \frac{1}{2}\ln\frac{\rho_{v,i} + \left(\bar{v}_i(t) - v_i(t)\right)}{\rho_{v,i} - \left(\bar{v}_i(t) - v_i(t)\right)} \le b_i \tag{14}$$

In addition, we can further obtain from (14) that:

$$-\rho_{v,i} \le \frac{\rho_{v,i} e^{-2b_i} - \rho_{v,i}}{e^{-2b_i} + 1} \le \bar{v}_i(t) - v_i(t) \le \frac{\rho_{v,i} e^{2b_i} - \rho_{v,i}}{e^{2b_i} + 1} \le \rho_{v,i} \tag{15}$$

From (15), we can observe that $\left|\bar{v}_i(t) - v_i(t)\right| \le \rho_{v,i}$, which indicates that the variations in the DCIG operating voltage are regulated by the prescribed dynamic performance.

Similarly, when $k_i P_i(t) - k_j P_j(t)$ is bounded, $\zeta_i(t)$ is bounded and we can obtain:

$$\left|\zeta_i(t)\right| \le c_i \tag{16}$$

where $c_i > 0$. Then, the following relationship is obtained as:

$$-\rho_{p,i} \le \frac{\rho_{p,i} e^{-2c_i} - \rho_{p,i}}{e^{-2c_i} + 1} \le \frac{1}{d_{ii}}\sum_{j=1}^{N} a_{ij}\left(k_i P_i(t) - k_j P_j(t)\right) \le \frac{\rho_{p,i} e^{2c_i} - \rho_{p,i}}{e^{2c_i} + 1} \le \rho_{p,i} \tag{17}$$

From (17), we can observe that $\left|\frac{1}{d_{ii}}\sum_{j=1}^{N} a_{ij}\left(k_i P_i(t) - k_j P_j(t)\right)\right| \le \rho_{p,i}$.

In other words, the variations in the DCIG power output are regulated to the prescribed dynamic performance. The proof is complete.

Based on Theorem 2, we can conclude that under the proposed control, the MG system is regulated to a prescribed transient-state performance, as the control objectives described in Section II-C are achieved.

V. Case Study

The performance of the proposed controller with the prescribed transient-state performance is validated via an islanded DC MG, as shown in Fig. 4. The test system is energized using four DCIGs with identical power capacities, and the developed CPS control framework is adopted. The power consumption at each bus is modeled as a constant resistive load. Notably, the proposed control is not limited to MG system topologies, where a DCIG must be connected to each bus, and is applicable to systems with constant power loads. Table I lists the detailed system parameter settings. For the control gains that can also be found in conventional SS-focused control, i.e., k_p, k_v, and k_V, their values can be designed by referring to the existing techniques [38]. For the control gains proposed in this paper that are dedicated to transient state regulation, i.e., α_1, β_i, γ_i, $\rho_{v,i}$, and $\rho_{p,i}$, their values can be designed with respect to the desired system transient-state performance with sufficient margin. As a proof of concept, it has been analytically proven that the MG under the proposed control is Lyapunov stable, i.e., the system convergence is guaranteed regardless of the control parameter selections. However, due to the practical limitations with respect to the operational safety of the DCIG, the control gains should be designed to be sufficiently small such that the device-level operating constraints at each DCIG are not vi-

olated.

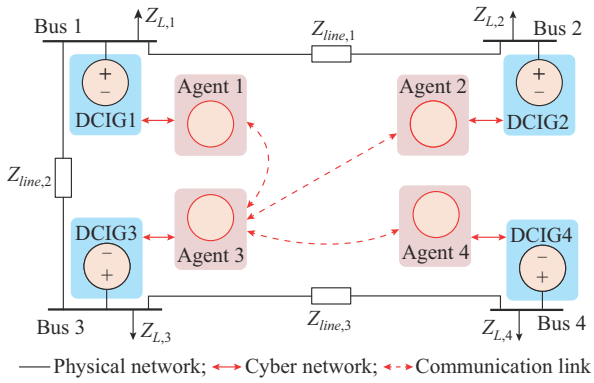

Fig. 4. Four-DCIG MG system with developed CPS control framework.

TABLE I
SYSTEM PARAMETER SETTING

Parameter	Value
Droop gain	$k_i = 5.4 \times 10^{-3}$ V/W
Rated voltage	$V^* = 380$ V
Power filter cut-off frequency	$\omega_0 = 2\pi$ rad/s
Resistance and inductance for transmission lines	$R_{line,1} = 0.35\ \Omega$, $L_{line,1} = 1.5$ mH, $R_{line,2} = 0.35\ \Omega$, $L_{line,2} = 1.5$ mH, $R_{line,3} = 0.35\ \Omega$, $L_{line,3} = 1.5$ mH
Resistance and inductance for resistive loads	$R_{L,1} = 15.625\ \Omega$, $R_{L,2} = 156.25\ \Omega$, $R_{L,3} = 62.5\ \Omega$, $R_{L,4} = 7.8\ \Omega$
Control gains ($i = 1, 2, 3, 4$)	$k_p = 0.05$, $k_v = 15$, $k_V = 1$, $\alpha_i = 10$, $\beta_i = 0.1$, $\gamma_i = 0.2$, $\rho_{v,i} = 1$, $\rho_{p,i} = 20$

A. Comparative Studies

In this scenario, the MG system initially operates in a steady state. At time instant $t_1 = 20$ s, part of the parallel load $\Delta R_L = 2R_{L,4}$ is disconnected from bus 4, which represents a 50% local load step-down at this bus. The MG system enters a transient state after the perturbation and eventually converges to a new steady state. The transient voltage dynamics at DCIG2 are recorded, as shown in Fig. 5. For comparison purposes, two additional scenarios are studied, where the DCIGs are equipped with $\dot{V}$-P droop and V-P droop at the primary level and the conventional SS-focused controller from [39] at the secondary level. As previously discussed, conventional SS-focused controllers typically adopt V-P droop at the primary level, whereas the proposed controller adopts $\dot{V}$-P droop. To better justify that the advanced transient-state performance of the proposed controller from the developed control in (2) and (3) over the $\dot{V}$-P droop at the primary level, the dynamic performance of the system under $\dot{V}$-P droop with a conventional SS-focused controller is also simulated for comparison. The MG system is perturbed by the same load variation, and the transient voltage dynamics at DCIG2 are shown in Fig. 5.

It can be observed from Fig. 5 that when the DCIGs are controlled by the conventional SS-focused controllers, even as the perturbed system gradually converges to a new steady-state operating point, significant transient voltages are generated at time instant t_1.

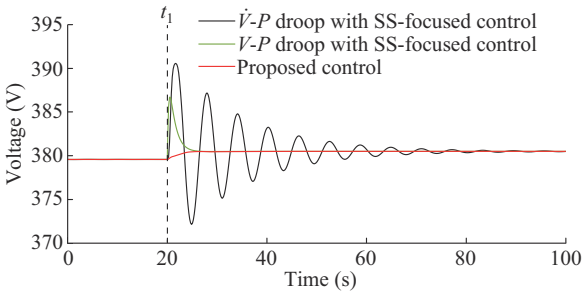

Fig. 5. Comparative transient voltage dynamics at DCIG2 under different controls.

Moreover, compared with the transients induced by V-P droop, those induced by $\dot{V}$-P droop are worse. However, when the DCIGs are implemented with the proposed controller, no significant transient voltage is observed, and the system seamlessly enters a new steady state. Further, the average DCIG voltage variations under different controls are presented in Fig. 6. It is observed that both the conventional SS-focused controller and the proposed controller achieve accurate average voltage regulations in the steady state. However, the transients are minimized when the proposed controller is implemented. Finally, the voltage regulation error $e_{v,i} = \bar{v}_i(t) - v_i(t)$ is recorded, as shown in Fig. 7. It is observed that under the proposed controller, this type of regulation error varies within the prescribed bound, as $|e_{v,i}| \rho_{v,i} = 1$ for $i = 1, 2, 3, 4$. The designed transient-state voltage control objective is achieved, as the designed constraints for the operating voltage are in compliance at each DCIG.

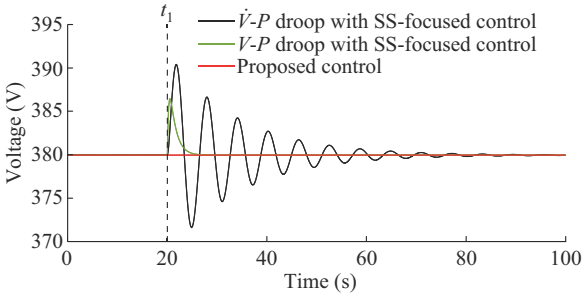

Fig. 6. Average DCIG voltage variations under different controls.

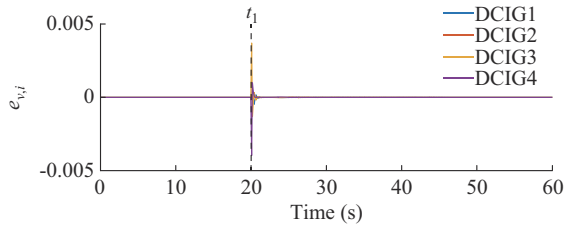

Fig. 7. $e_{v,i}$ under proposed control.

The power output variations of each DCIG under the proposed control are recorded, as shown in Fig. 8. It is observed from Fig. 8 that the power outputs of the DCIGs are regulated such that their mismatches are close to zero in the transient state, which agrees with the designed transient state control objectives. Moreover, accurate power-sharing regula-

tions are achieved in the steady state. The DCIG power-sharing regulation errors $e_{p,i}=\frac{1}{d_{ii}}\sum_{j=1}^{N}a_{ij}\left(k_iP_i(t)-k_jP_j(t)\right)$ are recorded, as shown in Fig. 9. It is observed from Fig. 9 that the power-sharing regulation error varies within the prescribed bound, i. e., $\left|e_{p,i}\right|\rho_{p,i}=20$ for $i=1,2,3,4$. The designed transient-state power control objective is achieved because the designed constraints for the power output are in compliance at each DCIG.

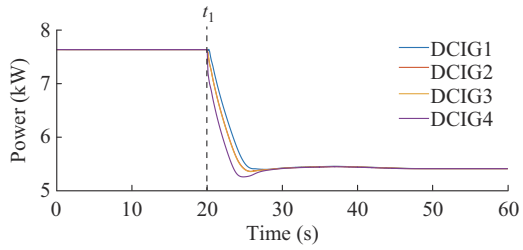

Fig. 8. DCIG power outputs under proposed control.

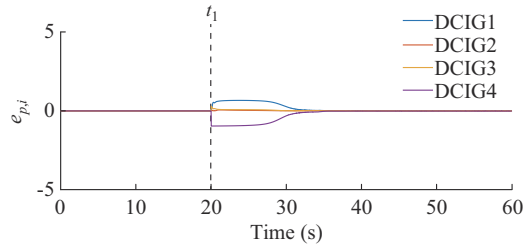

Fig. 9. $e_{p,i}$ under proposed control.

For comparison purposes, one additional scenario is studied, wherein the transient-state-focused voltage regulation is activated at each DCIG and the one for power-sharing regulation is disabled. In other words, for $i=1,2,3,4$, $u_i(t)$ is enabled and $d_i(t)=0$. The resulted DCIG power regulation errors are presented in Fig. 10. Compared with the results presented in Fig. 9, Fig. 10 shows that when $d_i(t)$ is disabled at each DCIG, significant variations of $e_{p,i}(t)$ are generated, which indicate a worse DCIG power-sharing performance. In other words, the transient-state-focused power-sharing regulation improves DCIG power-sharing performance in the transient state. Moreover, Figs. 9 and 10 show that a tradeoff exists between the overshoot and settling time of $e_{p,i}(t)$, i. e., the transient response and convergence time of the MG system. This is expected because the proposed controller focuses on restricting the system transients to be within a prescribed bound, which is at the expense of convergence time. Thus, although it has been observed that the system remains stable under different values of controller parameters, the transient-state performance of the system would vary, and the system parameters could be carefully designed to achieve desired system transient-state performance. This type of design objective requires sophisticated techniques, e. g., machine-learning-based approaches, and will be studied in a future work.

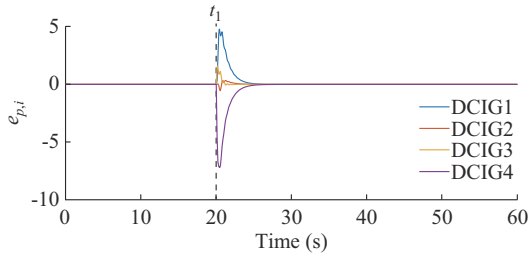

Fig. 10. $e_{p,i}$ when $d_i(t)=0$.

For further validation, the variations of $e_{p,i}(t)$ are studied under different selections of $\rho_{p,i}$, where the resulting $e_{p,i}$ at DCIG4 is shown in Fig. 11. Figure 11 shows that an increased value of $\rho_{p,i}$ (indicating relaxed transient-state-focused power-sharing regulation efforts) leads to a greater overshoot of $e_{p,4}$ but consumes less convergence time. Nevertheless, the variations of $e_{p,4}$ have always been regulated to the prescribed performance, and the effectiveness of the proposed controller has been validated.

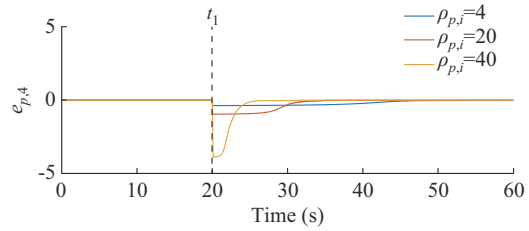

Fig. 11. Variations of $e_{p,4}$ under different selections of $\rho_{p,i}$.

B. Effectiveness of Proposed Control with Switching Communication Topologies and Various Load Disturbances

In this scenario, the communication topology switch due to communication failures is shown in Fig. 12. In addition, a 50% local load step-down is first introduced at bus 4, and a 66.6% local load step-up is then introduced at bus 1. The load variations at buses 4 and 1 are introduced at time instants t_2 and t_4, respectively, and the communication topology switch is introduced at time instant t_3.

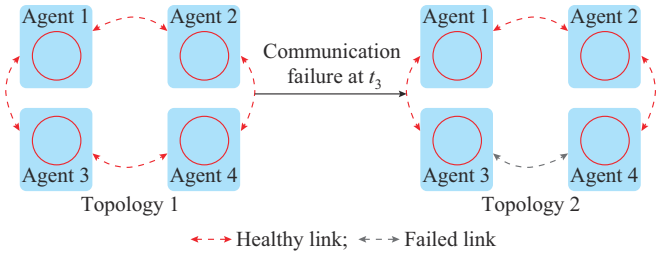

Fig. 12. Communication topology switch due to communication failure.

It is observed from Figs. 13 and 14 that at time instants t_2 and t_4, the developed steady-state and transient-state control objectives over the operating voltage at each DCIG are achieved under different communication topologies and load disturbances. In other words, the average voltage of the DCIGs is regulated as rated in the steady state, and the volt-

age regulation errors are well-bounded in the transient state. We conclude that the proposed control provides continuous regulations over the operating voltage of each DCIG, regardless of the communication topology or the location of load disturbances. With reference to Figs. 15 and 16, similar conclusions can be drawn regarding the effectiveness of the proposed control for DCIG power output regulation.

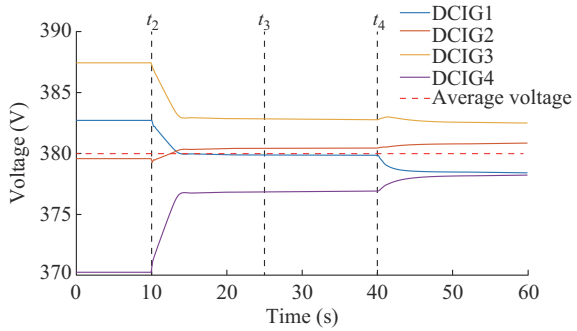

Fig. 13. DCIG voltage variations with switching communication topologies and various load disturbances under proposed control.

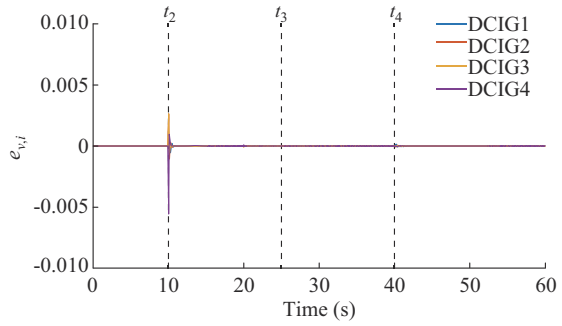

Fig. 14. $e_{v,i}$ with switching communication topologies and various load disturbances under proposed control.

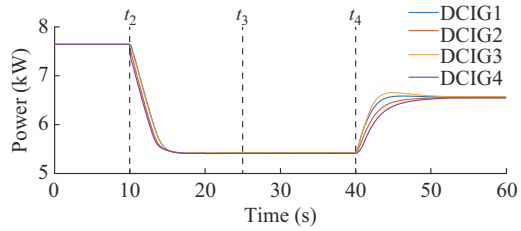

Fig. 15. DCIG power outputs with switching communication topologies and various load disturbances under proposed control.

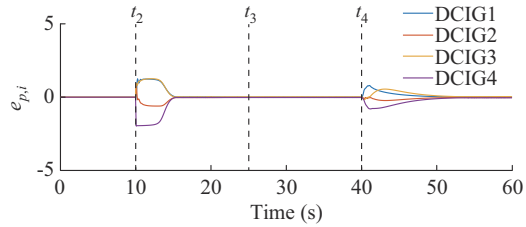

Fig. 16. $e_{p,i}$ with switching communication topologies and various load disturbances under proposed control.

C. Effectiveness of Proposed Control with DCIG Plug-and-play Capabilities

In this scenario, DCIG1 is first disconnected from the power grid, and the islanded MG is energized from DCIG2 to DCIG4. A 50% local load step-down is then introduced at bus 4 to validate the performance of the proposed controller when partial DCIGs are available. Finally, DCIG1 is reconnected to the power grid, and the four DCIGs are coordinated. DCIG1 is disconnected at time instant t_5 and reconnected at time instant t_7, as shown in Fig. 17, and the load variations at bus 4 are introduced at time instant t_6.

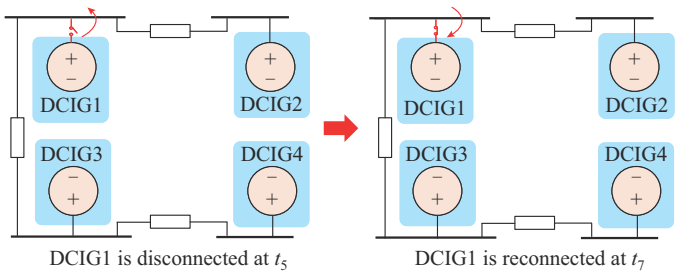

Fig. 17. System reconfiguration due to plug-and-play capabilities of DCIG1.

Figure 18 shows that the developed steady-state control objectives over the operating voltage at each DCIG have been achieved, as the average voltage of the DCIGs has been regulated as rated in the steady state. Notably, to ensure smooth reconnection, the operating voltage at DCIG1 remains unchanged after disconnection. In addition, during t_5 to t_7 when DCIG1 is disconnected, the average voltage of DCIG1 to DCIG4 deviates from the rated value, which is expected because the average voltages of DCIG2 to DCIG4 are under regulation during this period. We also observe that after DCIG1 is reconnected, the average voltages of DCIG1 to DCIG4 are regulated back to the rate, which validates the plug-and-play capabilities of the proposed controller. Figure 19 shows that the DCIG voltage regulation errors are well-bounded during the disconnection and reconnection of DCIG1, and the transient-state control objectives are achieved even when the system is energized by DCIG2 to DCIG4. The results shown in Fig. 19 validate the plug-and-play capabilities of the proposed controller in the transient state. With reference to the results in Figs. 20 and 21, similar conclusions can be drawn regarding the plug-and-play capabilities of the proposed controller in regulating the DCIG power output during both steady state and transient state.

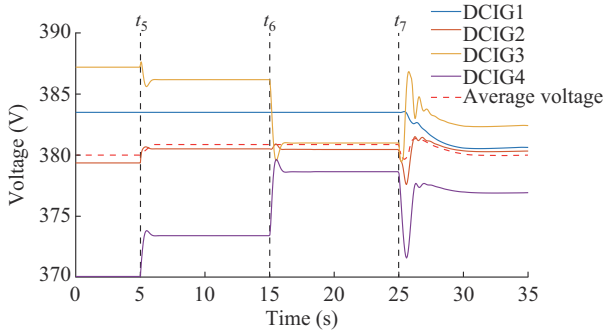

Fig. 18. DCIG voltage variations with plug-and-play capabilities of DCIG1 under proposed control.

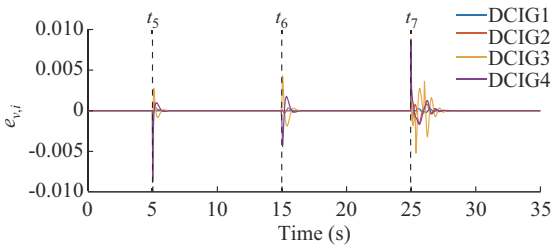

Fig. 19. $e_{v,i}$ with plug-and-play capabilities of DCIG1 under proposed control.

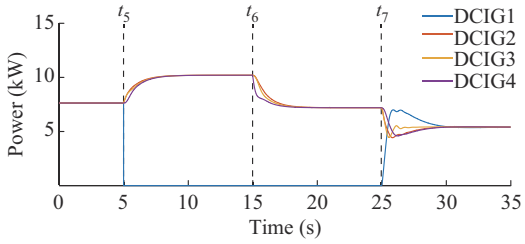

Fig. 20. DCIG power outputs with plug-and-play capabilities of DCIG1 under proposed control.

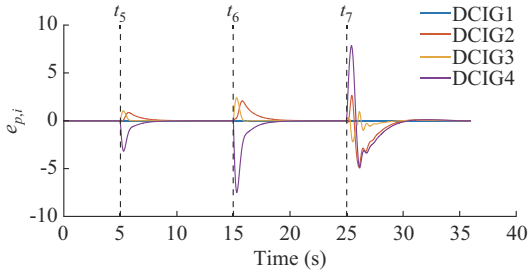

Fig. 21. $e_{p,i}$ with plug-and-play capabilities of DCIG1 under proposed control.

VI. Conclusion

A set of distributed controllers is introduced in this paper that considers both steady-state and transient-state performances of an islanded DC MG. The proposed control achieves not only accurate secondary regulations in the steady state but also controls the system operating states to the prescribed transient-state performance. A CPS control framework with extended control flexibility is developed and the conventional PPC is modified to cope with the practical operating characteristics of the MG system. The MG system under control is proven to be Lyapunov stable using large-signal stability analysis, and both the steady- and transient-state performances of the system are analyzed. This paper rigorously proves that the proposed control achieves accurate DCIG average voltage and proportional power-sharing regulations in the steady state, and the variations in the DCIG operating voltage and power output are regulated as prescribed. The effectiveness of the proposed control is validated via a four-DCIG MG system.

References

[1] Z. Li, Z. Cheng, J. Si *et al*., "Distributed event-triggered secondary control for average bus voltage regulation and proportional load sharing of DC microgrid," *Journal of Modern Power Systems and Clean Energy*, vol. 10, no. 3, pp. 678-688, May 2022.

[2] Y. Du, X. Lu, J. Wang *et al*., "Distributed secondary control strategy for microgrid operation with dynamic boundaries," *IEEE Transactions on Smart Grid*, vol. 10, no. 5, pp. 5269-5282, Sept. 2019.

[3] J. Yang and Y. Zhang, "A privacy-preserving algorithm for ac microgrid cyber-physical system against false data injection attacks," *Journal of Modern Power Systems and Clean Energy*, vol. 11, no. 5, pp. 1646-1658, Sept. 2023.

[4] Z. Cheng, J. Duan, and M.-Y. Chow, "To centralize or to distribute: that is the question: a comparison of advanced microgrid management systems," *IEEE Industrial Electronics Magazine*, vol. 12, no. 1, pp. 6-24, Mar. 2018.

[5] Y. Khayat, Q. Shafee, R. Heydari *et al*., "On the secondary control architectures of AC microgrids: an overview," *IEEE Transactions on Power Electronics*, vol. 35, no. 6, pp. 6482-6500, Jun. 2020.

[6] J. Duan, C. Wang, H. Xu *et al*., "Distributed control of inverter-interfaced microgrids based on consensus algorithm with improved transient performance," *IEEE Transactions on Smart Grid*, vol. 10, no. 2, pp. 1303-1312, Mar. 2019.

[7] A. Hirsch, Y. Parag, and J. Guerrero, "Microgrids: a review of technologies, key drivers, and outstanding issues," *Renewable and Sustainable Energy Reviews*, vol. 90, pp. 402-411, Jul. 2018.

[8] Y. Yu, L. Quan, Z. Mi *et al*., "Improved model predictive control with prescribed performance for aggregated thermostatically controlled loads," *Journal of Modern Power Systems and Clean Energy*, vol. 10, no. 2, pp. 430-439, Mar. 2022.

[9] H. Xu, C. Yu, C. Liu *et al*., "An improved virtual inertia algorithm of virtual synchronous generator," *Journal of Modern Power Systems and Clean Energy*, vol. 8, no. 2, pp. 377-386, Mar. 2020.

[10] Y. Wang, F. Qiu, G. Liu *et al*., "Adaptive reference power based voltage droop control for VSC-MTDC systems," *Journal of Modern Power Systems and Clean Energy*, vol. 11, no. 1, pp. 381-388, Jan. 2023.

[11] H. Wu and X. Wang, "Design-oriented transient stability analysis of PLL-synchronized voltage-source converters," *IEEE Transactions on Power Electronics*, vol. 35, no. 4, pp. 3573-3589, Apr. 2020.

[12] C. Shen, Z. Shuai, Y. Shen *et al*., "Transient stability and current injection design of paralleled current-controlled VSCs and virtual synchronous generators," *IEEE Transactions on Smart Grid*, vol. 12, no. 2, pp. 1118-1134, Mar. 2021.

[13] B. She, F. Li, H. Cui *et al*., "Inverter PQ control with trajectory tracking capability for microgrids based on physics-informed reinforcement learning," *IEEE Transactions on Smart Grid*, vol. 15, no. 1, pp. 99-112, Jan. 2024.

[14] J. M. Rey, M. Castilla, J. Miret *et al*., "Adaptive slope voltage control for distributed generation inverters with improved transient performance," *IEEE Transactions on Energy Conversion*, vol. 34, no. 3, pp. 1644-1654, Sept. 2019.

[15] J. Ye, L. Liu, J. Xu *et al*., "Frequency adaptive proportional-repetitive control for grid-connected inverters," *IEEE Transactions on Industrial Electronics*, vol. 68, no. 9, pp. 7965-7974, Sept. 2021.

[16] F. Gao, R. Kang, J. Cao *et al*., "Primary and secondary control in dc microgrids: a review," *Journal of Modern Power Systems and Clean Energy*, vol. 7, no. 2, pp. 227-242, Mar. 2019.

[17] X. Wang, X. Dong, X. Niu *et al*., "Toward balancing dynamic performance and system stability for DC microgrids: a new decentralized adaptive control strategy," *IEEE Transactions on Smart Grid*, vol. 13, no. 5, pp. 3439-3451, Sept. 2022.

[18] T. Shi, X. Xiang, J. Lei *et al*., "Communication-less active damping method with VSC for stability improvement of grid-connected DC microgrid with selected frequency islanding detection," *IEEE Transactions on Industrial Electronics*, vol. 71, no. 10, pp.1-11, Oct. 2024.

[19] M. Zhang, Q. Xu, C. Zhang *et al*., "Decentralized coordination and stabilization of hybrid energy storage systems in DC microgrids," *IEEE Transactions on Smart Grid*, vol. 13, no. 3, pp. 1751-1761, May 2022.

[20] C. Wang, J. Duan, B. Fan *et al*., "Decentralized high-performance control of DC microgrids," *IEEE Transactions on Smart Grid*, vol. 10, no. 3, pp. 3355-3363, May 2019.

[21] J. Peng, B. Fan, J. Duan *et al*., "Adaptive decentralized output-constrained control of single-bus DC microgrids," *IEEE/CAA Journal of Automatica Sinica*, vol. 6, no. 2, pp. 424-432, Mar. 2019.

[22] N. Sarrafan, M.-A. Rostami, J. Zarei *et al*., "Improved distributed prescribed finite-time secondary control of inverter-based microgrids: design and real-time implementation," *IEEE Transactions on Industrial Electronics*, vol. 68, no. 11, pp.11135-11145, Nov. 2021.

[23] S. Huang, J. Wang, L. Xiong *et al*., "Distributed predefned-time fractional-order sliding mode control for power system with prescribed

tracking performance," *IEEE Transactions on Power Systems*, vol. 37, no. 3, pp. 2233-2246, May 2022.
[24] Q. Geng, H. Sun, X. Zhou *et al*., "A storage-based fixed-time Grid and frequency synchronization method for improving transient stability and resilience of smart grid," *IEEE Transactions on Smart Grid*, vol. 14, no. 6, pp. 1-1, Nov. 2023.
[25] Y. Xia, W. Wei, T. Long *et al*., "New analysis framework for transient stability evaluation of DC microgrids," *IEEE Transactions on Smart Grid*, vol. 11, no. 4, pp. 2794-2804, Jul. 2020.
[26] X. Li, J. Zhang, Z. Tian *et al*., "Transient stability analysis of converter-based islanded microgrids dynamics and varying damping," *Journal of Modern Power Systems and Clean Energy*, vol. 12, no. 4, pp. 1-12, Jul. 2023.
[27] Y. Shen, Y. Peng, Z. Shuai *et al*., "Hierarchical time-series assessment and control for transient stability enhancement in islanded microgrids," *IEEE Transactions on Smart Grid*, vol. 14, no. 5, pp. 3362-3374, Sept. 2023.
[28] J. Peng, B. Fan, and W. Liu, "Voltage-based distributed optimal control for generation cost minimization and bounded bus voltage regulation in DC microgrids," *IEEE Transactions on Smart Grid*, vol. 12, no. 1, pp. 106-116, Jan. 2021.
[29] R. Han, H. Wang, Z. Jin *et al*., "Compromised controller design for current sharing and voltage regulation in DC microgrid," *IEEE Transactions on Power Electronics*, vol. 34, no. 8, pp. 8045-8061, Aug. 2019.
[30] S. Sahoo, D. Pullaguram, S. Mishra *et al*., "A containment based distributed finite-time controller for bounded voltage regulation proportionate current sharing in DC microgrids," *Applied Energy*, vol. 228, pp. 2526-2538, Oct. 2018.
[31] Q. Yuan, Y. Wang, X. Liu *et al*., "Prescribed performance-based secondary control for DC microgrid," *IEEE Transactions on Energy Conversion*, vol. 37, no. 4, pp. 2610-2619, Dec. 2022.
[32] C. Zhang, X. Dou, X. Quan *et al*., "Distributed secondary control for island microgrids with expected dynamic performance under communication delays," *IEEE Transactions on Smart Grid*, vol. 14, no. 3, pp. 2010-2022, May 2023.
[33] J. W. Simpson-Porco, Q. Shafee, F. Do¨rfer *et al*., "Secondary frequency and voltage control of islanded microgrids via distributed averaging," *IEEE Transactions on Industrial Electronics*, vol. 62, no. 11, pp. 7025-7038, Nov. 2015.
[34] J. Zhao and F. Dörfer, "Distributed control and optimization in DC microgrids," *Automatica*, vol. 61, pp. 18-26, Nov. 2015.
[35] D. P. Spanos, R. Olfati-Saber, and R. M. Murray, "Dynamic consensus on mobile networks," in *IFAC World Congress*. Prague: Czech Republic, 2005.
[36] C. P. Bechlioulis and G. A. Rovithakis, "Robust adaptive control of feedback linearizable MIMO nonlinear systems with prescribed performance," *IEEE Transactions on Automatic Control*, vol. 53, no. 9, pp. 2090-2099, Oct. 2008.
[37] H. Tu, H. Yu, Y. Du *et al*., "An IoT-based framework for distributed generic microgrid controllers," *IEEE Transactions on Control Systems Technology*, vol. 32, no. 5, pp. 1-14, Sept. 2024.
[38] Y. Du, X. Lu, and W. Tang, "Accurate distributed secondary control for DC microgrids considering communication delays: a surplus consensus-based approach," *IEEE Transactions on Smart Grid*, vol. 13, no. 3, pp. 1709-1719, May 2022.
[39] V. Nasirian, S. Moayedi, A. Davoudi *et al*., "Distributed cooperative control of DC microgrids," *IEEE Transactions on Power Electronics*, vol. 30, no. 4, pp. 2288-2303, Apr. 2015.

Aili Fan received the Ph.D. degree from Xidian University, Xi'an, China, in 2020. Since 2021, she has been an Associate Professor with Northwestern Polytechnical University, Xi'an, China. Her research interests include learning control of multiagent system, robust control, complex network synchronization, and neural network control.

Jiangong Yang received the B. S. degree in electrical engineering from Northwestern Polytechnical University, Xi'an, China, in 2021, where he is currently pursuing the M.S. degree in electrical engineering. His research interests include microgrid virtual inertia control and microgrid distributed control.

Yuhua Du received the B.S. degree in electrical engineering from Xi'an Jiaotong University, Xi'an, China, in 2013, and the Ph.D. degree in electrical and computer engineering from North Carolina State University, Raleigh, USA, in 2019. He was a Research Aide with Argonne National Laboratory, DuPage County, USA, in 2018. In February 2022, he was with the School of Automation, Northwestern Polytechnical University, Xi'an, China, as a Professor. His research interests include voltage source converter modeling and control, microgrid distributed control, and microgrid hardware-in-the-loop testbed.

Zhipeng Li received the bachelor's degree in physics from Beijing Normal University, Beijing, China, and the doctoral degree in materials science and engineering from the National University of Singapore, Singapore. He has studied and worked abroad for nearly 20 years and has served as a Senior Researcher at the National Institute of Materials Research and Engineering in Singapore, the National Institute of Materials Research in Japan, and the National Bureau of Standards in the USA. Subsequently, he engaged in industrialized high-end manufacturing in the first-line industry in Silicon Valley, and served as the Principal Engineer and Project Leader in the world's top 500 enterprises. He is now the Director of the Zero Carbon Science and New Energy Technology Center in Institute of Flexible Electronics of Northwestern Polytechnical University, Xi'an, China. His research interests include cutting-edge core technology of new energy fuel cells and industrial manufacturing, especially first-line technology of industrialization.

Fei Gao received the Ph.D. degree in Renewable Energy from the University of Technology of Belfort-Montbéliard (UTBM), Belfort, France, in 2010. He now serves as the Executive Director of Research, Doctoral Studies, and Innovation at UTBM, and is also a Full Professor at UTBM. His research interests include hydrogen fuel cells for transportation and digital twin technology in modern power electronics and energy systems.

Yigeng Huangfu received the M.S. and Ph.D. degrees in electrical engineering from Northwestern Polytechnical University, Xi'an, China, in 2007 and 2009, respectively. He also received the Ph.D. degree from the University of Technology of Belfort-Montbeliard, Belfort, France, in 2010. He has been the Professor at Northwestern Polytechnical University. His research interests include power electrical conversion, transportation electrification, control of new energy conversion and renewable energy generation technology.